Electronic Supplementary Material (ESI) for Journal of Materials Chemistry A.

Supporting Information

Enhanced Electroreduction of CO_2 by Ni–N–C Catalysts from the Interplay Between Valency and Local Coordination Symmetry

*Dongyup Shin,[a] Hansol Choi,[b] Jihun An,[a] Chang Ho Sohn, [c,d] Chang-Hyuck Choi,[c] Hyeyoung Shin,[*f] and Hyungjun Kim[*a]*

[a]Department of Chemistry, Korea Advanced Institute of Science and Technology, Daejeon 34141, Republic of Korea.

[b]School of Materials Science and Engineering, Gwangju Institute of Science and Technology, Gwangju 61005, Republic of Korea.

[c]Department of Chemistry, Pohang University of Science and Technology, Pohang 37673, Republic of Korea.

[d]Graduate Program of Nano Biomedical Engineering (NanoBME), Advanced Science Institute, Yonsei University, Seoul, 03722, Republic of Korea.

[e]Department of Chemistry, Pohang University of Science and Technology, Pohang 37673, Republic of Korea

[f]Graduate School of Energy Science and Technology (GEST), Chungnam National University, Daejeon 34134, Republic of Korea.

*Corresponding authors: (H. Kim) linus16@kaist.ac.kr (H. Shin) shinhy@cnu.ac.kr

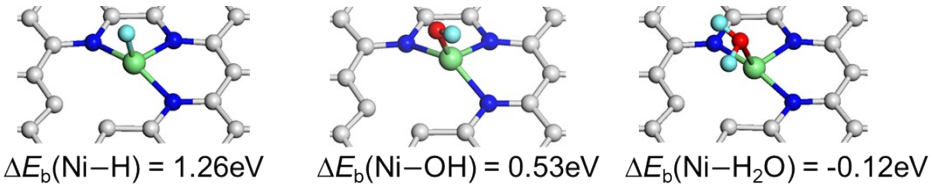

Fig. S1 DFT-calculated structures and energies of H, OH, and H_2O absorbed Ni−N_3V system. The grey, blue, red, light-green and cyan spheres represent carbon, nitrogen, oxygen, nickel and hydrogen atoms, respectively. The adsorption energy (ΔE_{ads}) of each adsorbate are computed as the following steps: $\Delta E_{ads.H} = E$(H-Ni−Ni_3V) − E(Ni−N_3V) − 1/2E(H_2), $\Delta E_{ads.OH}$ = E(OH-Ni−Ni_3V) − E(Ni−N_3V) − E(H_2O) + 1/2E(H_2), and $\Delta E_{ads.H2O}$ = E(H_2O-Ni−Ni_3V) − E(Ni−N_3V) − E(H_2O). Note that the $\Delta E_{ads.}$ does not include an entropic contribution. For example, a dramatic entropic cost is expected for the binding of liquid water ($S_{wat(liq.)}$ = 69.9 J K^{-1} mol^{-1}, converting into the free energy cost of 0.22 eV at 300K).

Comment [□]: C-H 계산 데이터 논의 후 수정 필요. 일단은 리뷰어2의 3번째 질문 답을 복붙해두었음.

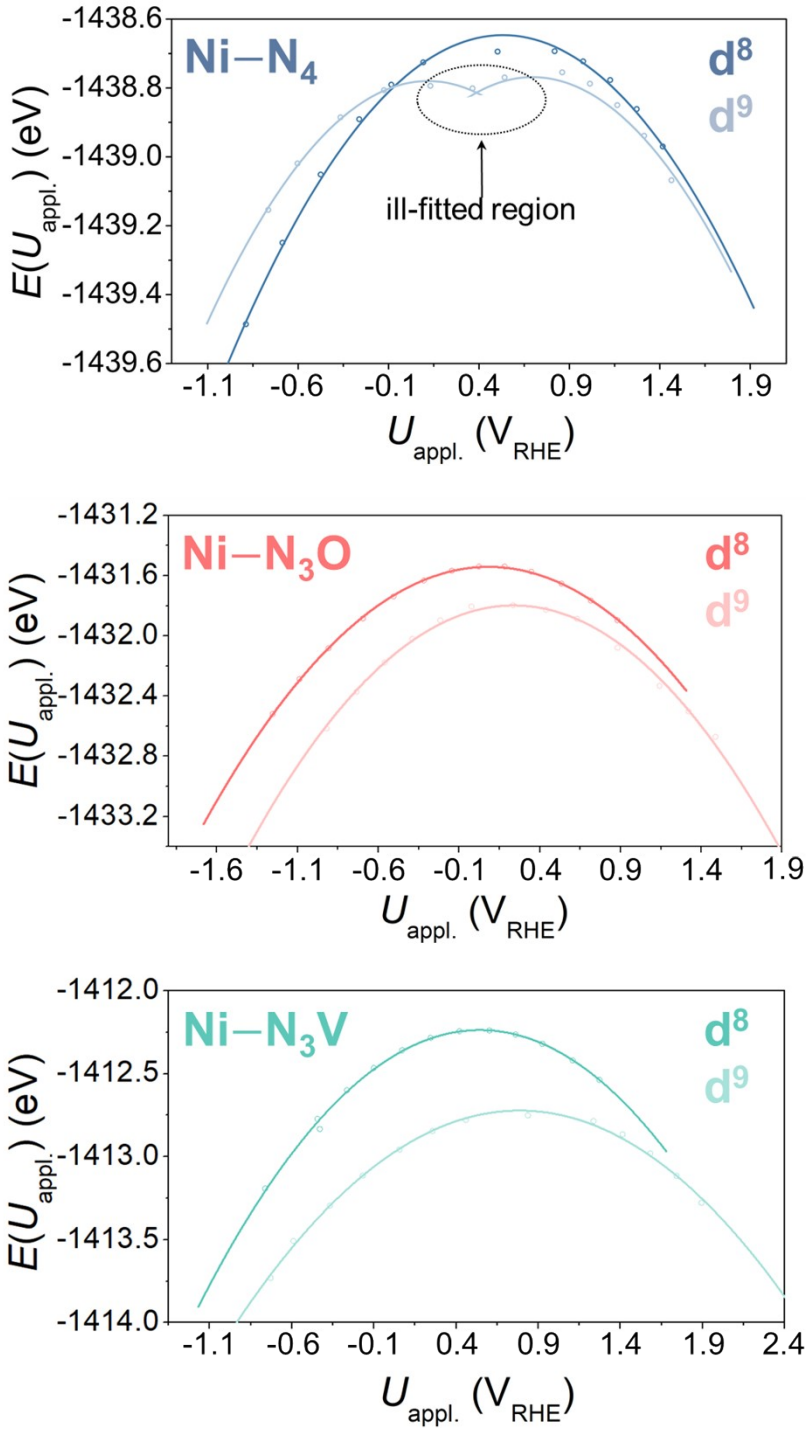

Fig. S2 Grand-canonical energy profiles versus RHE (pH = 6.8) of Ni–N_4, Ni–N_3O, and Ni–N_3V systems with two different Ni oxidation states—Ni^{2+} and Ni^{1+}—are compared.

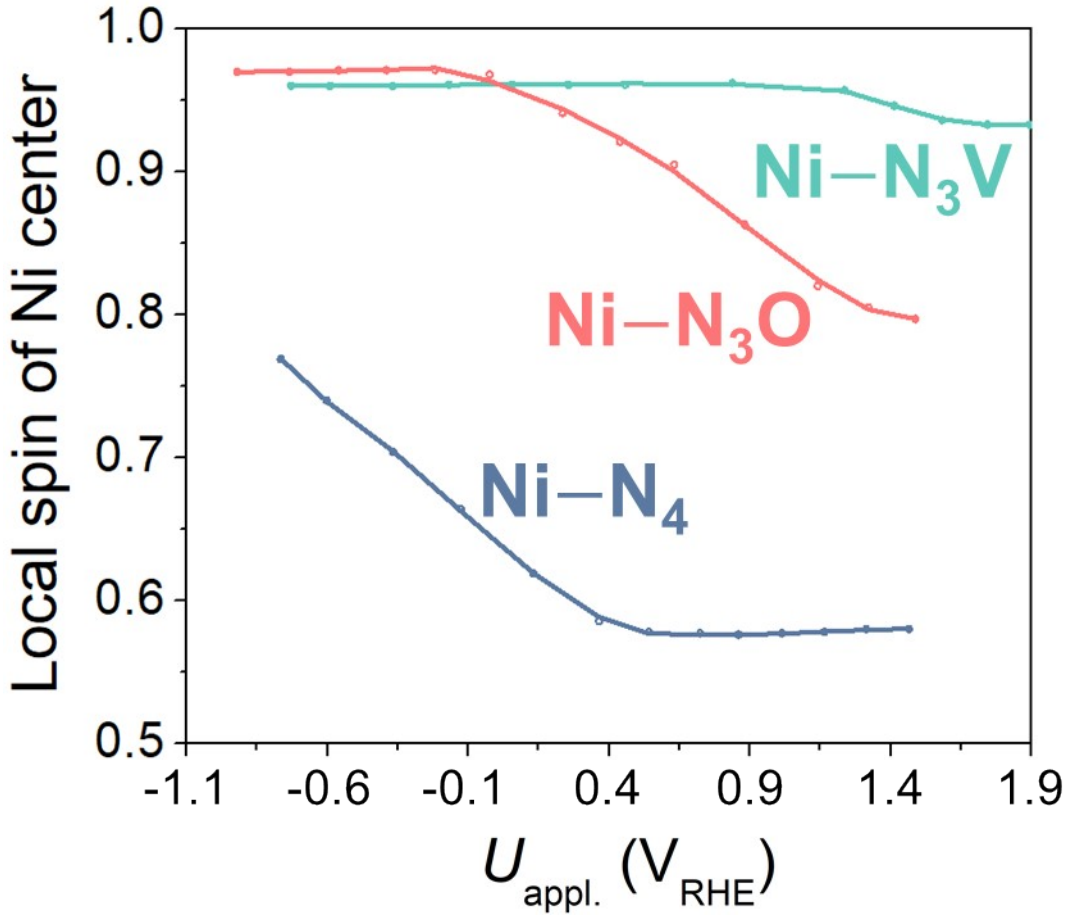

Fig. S3 Change of local spin (*S*) at the Ni^{1+} center for Ni–N_4 (blue), Ni–N_3O (coral), and Ni–N_3V (green) systems with RHE (pH = 6.8).

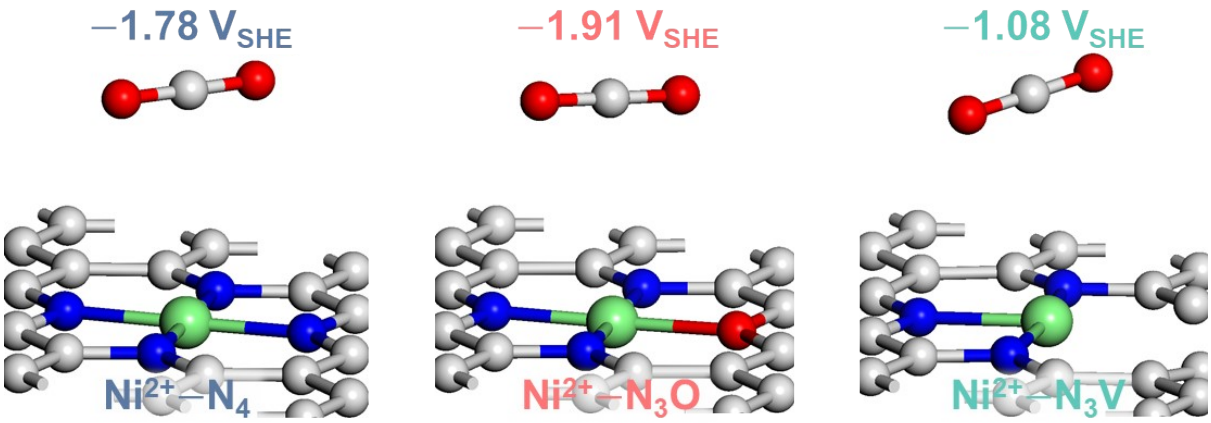

Fig. S4 DFT-calculated geometry of the CO_2 adsorption step on the Ni^{2+} sites. Each simulation cell had an excess charge corresponding to -2.0 *e*, and the potentials versus SHE (V_{SHE}) corresponding to the excess charge were specified.

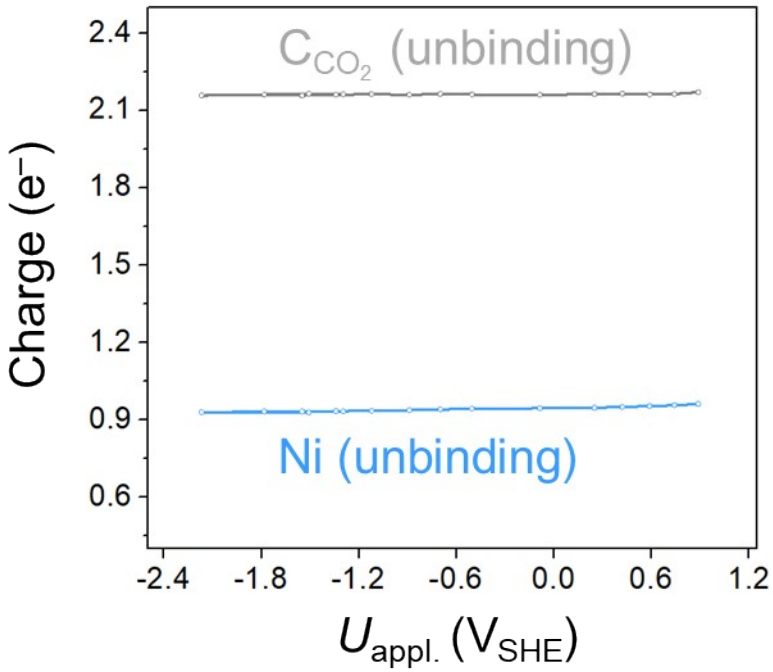

Fig. S5 Change of partial charges on the Ni center (blue) and C atom of the CO_2 (grey) depending on the applied potential U_{appl}. No charge transfer is observed between Ni^{2+} and CO_2.

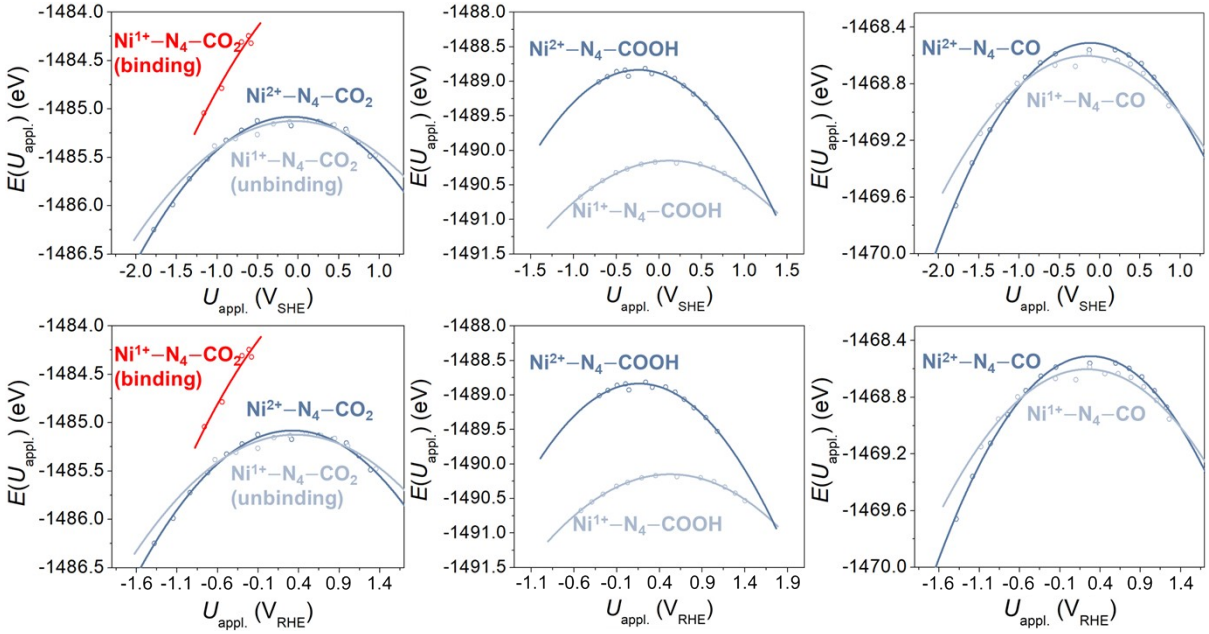

Fig. S6 Grand-canonical energy profiles versus SHE (first row) and RHE (second row, at pH = 6.8) of the CO_2, COOH, and CO intermediates adsorbed on the Ni–N_4 system.

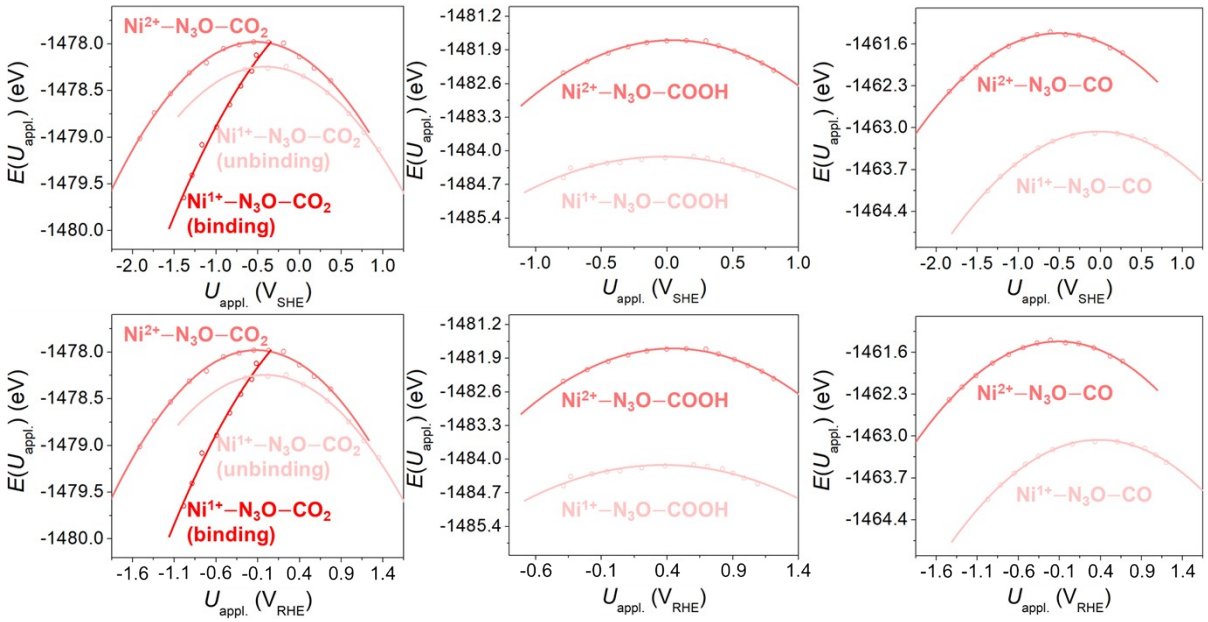

Fig. S7 Grand-canonical energy profiles versus SHE (first row) and RHE (second row, at pH = 6.8) of the CO_2, COOH, and CO intermediates adsorbed on the Ni–N_3O system.

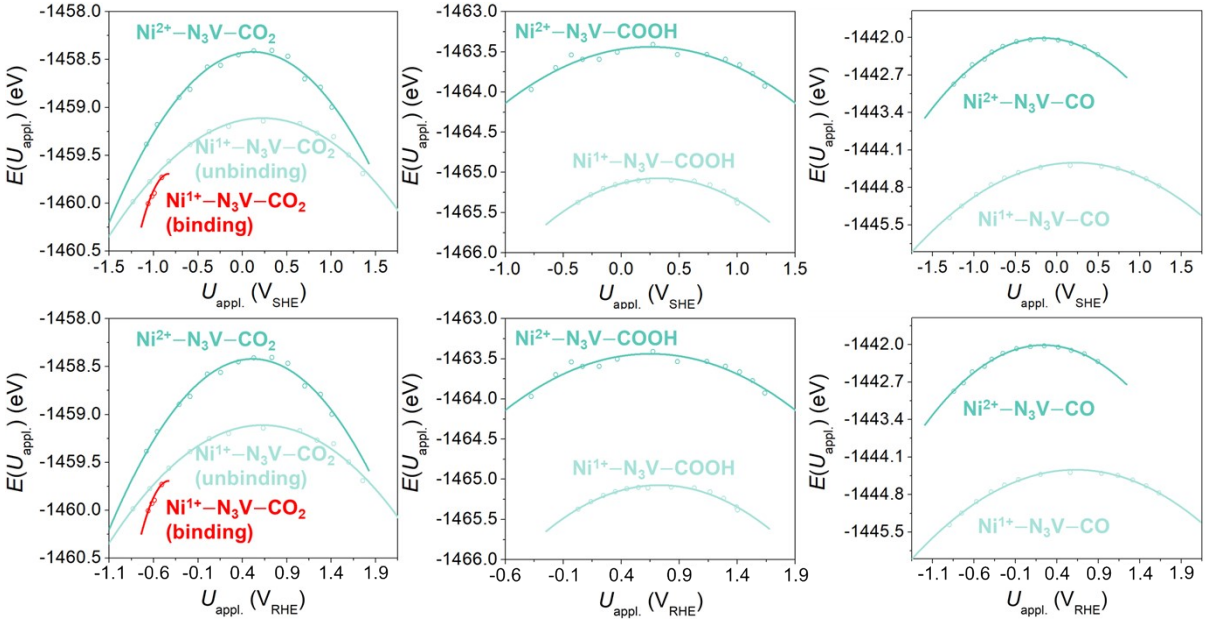

Fig. S8 Grand-canonical energy profiles versus SHE (first row) and RHE (second row, at pH = 6.8) of the CO_2, COOH, and CO intermediates adsorbed on the Ni–N_3V system.